Annu. Rev. Biophys. Biomol. Struct. 1997. 26:541–66

USE OF SURFACE PLASMON RESONANCE TO PROBE THE EQUILIBRIUM AND DYNAMIC ASPECTS OF INTERACTIONS BETWEEN BIOLOGICAL MACROMOLECULES[1]

Peter Schuck

Section of Physical Biochemistry, Laboratory of Biochemical Pharmacology, National Institute of Diabetes, Digestive, and Kidney Diseases, National Institutes of Health,[2] Bethesda, Maryland 20892; email: pschuck@helix.nih.gov

KEY WORDS: evanescent wave biosensor, grating coupler sensor, resonant mirror, reversible interactions, binding kinetics

ABSTRACT

Surface plasmon resonance biosensors have become increasingly popular for the qualitative and quantitative characterization of the specific binding of a mobile reactant to a binding partner immobilized on the sensor surface. This article reviews the use of this new technique to measure the binding affinities and the kinetic constants of reversible interactions between biological macromolecules. Immobilization techniques, the most commonly employed experimental strategies, and various analytical approaches are summarized. In recent years, several sources of potential artifacts have been identified: immobilization of the binding partner, steric hindrance of binding to adjacent binding sites at the sensor surface, and finite rate of mass transport of the mobile reactant to the sensor surface. Described here is the influence of these artifacts on the measured binding kinetics and equilibria, together with suggested control experiments.

[2]Present address: Biomedical Engineering and Instrumentation Program, National Center for Research Resources, NIH.

CONTENTS

INTRODUCTION

With the introduction of a commercial surface plasmon resonance (SPR) biosensor in 1990, optical evanescent wave biosensors have become readily available and increasingly popular as a tool for the quantitative and qualitative characterization of reversible interactions between biological macromolecules. In contrast to solution methods, these biosensors can detect specific reversible binding of a reactant in a mobile phase to a binding partner immobilized on the surface of the sensor. SPR biosensors are attractive in part because the measured physical quantity is a refractive index change and, therefore, no chromophoric group or labeling of the macromolecules is required. In addition, the SPR biosensor provides real-time information on the course of the binding, it can be applied to interactions within a broad range of affinities (μM to sub-nM), and it uses small sample volumes with, in general, comparatively low requirements on the purity of one of the reactants.

Currently, several hundred studies on macromolecular interactions using SPR (and related) biosensors have been published in a broad variety of fields. These include cell adhesion molecules (109, 110), T-cell antigen-receptor and MHC-encoded molecules (1, 6, 12, 53, 61, 63, 65), receptor-ligand interactions (13, 41), signal transduction (20, 56, 67, 82), antibody-antigen interactions and antibody engineering (38, 52, 64, 73, 81), virus research (28, 83, 90, 112), protein-carbohydrate interactions (62), protein-DNA and DNA-DNA interactions (2, 5, 7, 22, 30, 115), interactions involving lipid vesicles or planar bilayers (55, 66, 87, 89, 94), and the assembly of a membrane-bound quaternary signal transduction complex (100). Apart from the commercial SPR biosensors [those made by Biacore, Uppsala, Sweden (BIAcore); and Intersens Instruments BV, Amersfoort, Netherlands (IBIS) (18, 59, 108)] and several laboratory-built SPR instruments (16, 39, 93, 95), two other types of commercial evanescent wave

biosensors are currently in use. These are based on resonant mirror principles [Affinity Sensors, Cambridge, UK (IAsys) (14)] or grating coupler principles [Artificial Sensing Instruments ASI AG, Zürich, Switzerland (BIOS-1) (4, 107)], and are similar to SPR biosensors in their functionality for the characterization of reversible interactions (4, 37, 75, 116).

The strategy used in a typical SPR biosensor experiment follows these steps: First, one reactant is covalently attached to the sensor surface. Then, in the association phase of the experiment, a mobile second reactant at constant concentration is introduced into the buffer flow above the sensor surface, and the progress of complex formation at the sensor surface is monitored. This procedure is followed by the dissociation phase, in which the free mobile reactant is absent from the buffer and the time-course of complex dissociation is recorded. Finally, the sensor surface is regenerated [for example by a short exposure to a buffer at low pH (49)] to remove the remaining complex. The cycle of association experiment, dissociation experiment, and regeneration is repeated using different concentrations of the mobile reactant. The obtained sequence of binding-progress curves (Figure 1) contains information on the

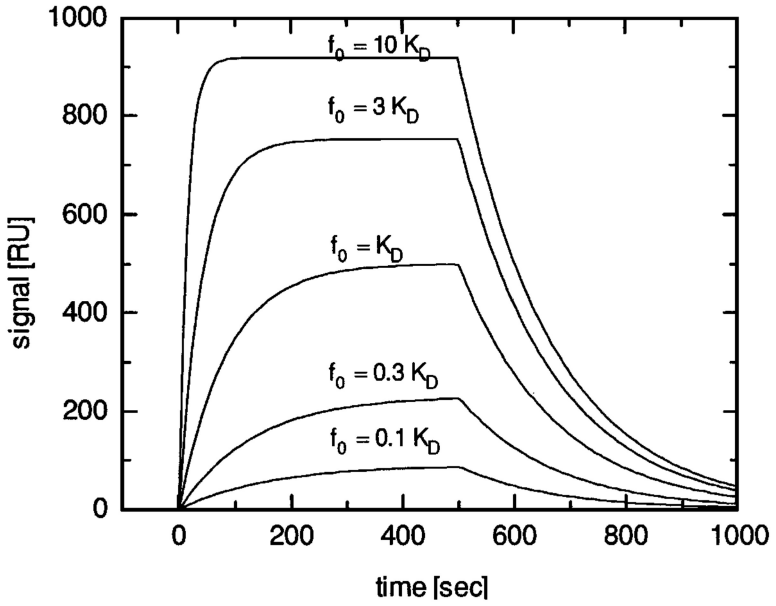

Figure 1 Schematic graph showing surface plasmon resonance biosensor signal expected for a simple 1:1 interaction with binding kinetics of pseudo-first-order. Superposition of the expected signal for different concentrations of mobile reactant. Association phase from 0–500 s, followed by a dissociation phase from 500–1000 s.

chemical rate constants and on the thermodynamic equilibrium constant of the interaction.

The use of evanescent wave biosensors for the reliable quantitative characterization of chemical binding kinetics and equilibria, in contrast to the usually straightforward qualitative analyses of binding, is a very demanding task, even for reactions that obey simple pseudo-first-order kinetics. The following difficulties have to be overcome: 1. the immobilization technique must attach the immobile reactant in a native conformation and, in a uniformly reactive and accessible orientation, to a surface that does not allow for a significant amount of nonspecific binding; 2. the relatively small refractive index increments of most biological macromolecules make it necessary to have a high local concentration of binding sites at the sensor surface (typically on the order of 10–100 μM within an immobilization matrix); and (3) the mobile reactant has to be efficiently transported to and from the reactive sensor surface, which is much more difficult than the mixing of reactants in solution is. As a consequence, the measured binding-progress curves potentially are governed by limitations in the mass transport of the mobile reactant to and from the sensor surface and by problems of steric hindrance of the neighboring binding sites at the sensor surface. These binding-progress curves also may suffer from the superposition of binding processes to different subpopulations of immobilized reactants and from nonspecific binding. In recent years, significant progress has been made in the development of experimental techniques for the solution or the minimization of these problems, in the design of control experiments, and in the development of analytical procedures to diagnose and account for these effects.

Since this technique has proven extremely versatile, the present review focuses on the main strategies for the use of SPR biosensors as a new tool for the analysis of equilibrium and kinetic rate constants of reversible interactions of biological macromolecules. Specific applications to different fields have been reviewed recently (64, 65, 109). See (25) for a review of the physical principles and the optical design of optical evanescent wave methods.

OPTICAL CONFIGURATION AND DETECTION PRINCIPLES

The basic optical configuration of an SPR biosensor consists of a prism coated with a thin metal film (usually silver or gold) (Figure 2). In this configuration, which was originally proposed by Kretschmann & Raether (54), the total internal reflection of light is used to excite nonradiative surface plasmons in the metal film. Surface plasmons are waves of oscillating surface charge density traveling along the metal surface. The electromagnetic field amplitudes

of nonradiative surface plasmons decay exponentially with increasing distance perpendicular to the sensor surface, with a decay length in the biosensor of a few hundred nanometers. These plasmons can be resonantly excited by light only at a well-defined angle of incidence, which occurs when the wave vector of the light in the plane of the sensor surface matches that of the surface plasmon. The resonance causes an energy loss in the reflected light, which is visible as a sharp minimum in the angle-dependent reflectance, which is, experimentally, the primary recorded quantity. The resonance angle strongly depends on the refractive index (or dielectric constant) profile of the sample within the evanescent field above the sensor surface. Adsorption or desorption of macromolecules at the sensor surface change the local refractive index and produce a shift in the resonance angle, which, to a good approximation, has been shown to be proportional to the surface concentration of macromolecules up to a concentration of 50 ng mm^{-2} (25, 105). For a given refractive index increment of the macromolecules, the signal is approximately proportional to the mass that is bound to the sensor surface. This imposes a lower limit on the molar mass of the mobile reactant to be detected in SPR biosensor experiments. Details of the physics and optical design involved in SPR instruments can be found elsewhere (25, 85). Other optical evanescent wave biosensors, such as resonant mirror sensors or grating couplers, do not exploit surface plasmons. They are based on waveguide principles and have a different optical configuration. However, they also detect changes in the refractive index of the solution above the sensor surface, within the evanescent field of light in total internal reflection (4, 14, 25, 89, 107).

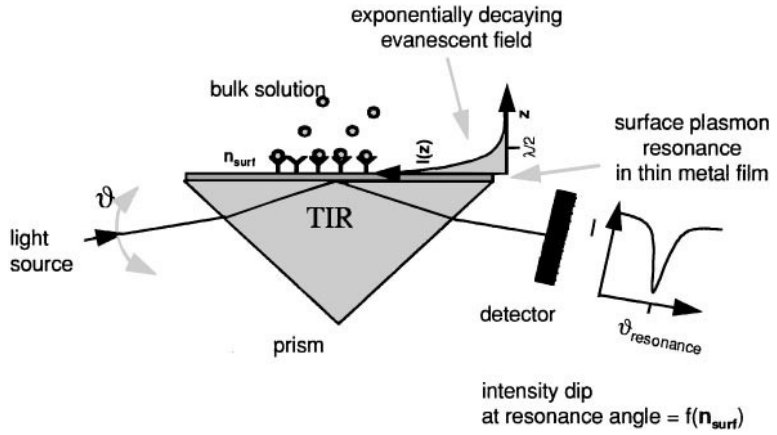

Figure 2 Schematic diagram of the setup of a surface plasmon resonance biosensor (TIR: total internal reflection; n_{surf}: refractive index of the bulk solution in the vicinity of the sensor surface).

The time-dependent change of the refractive index in the vicinity of the surface upon binding is commonly measured in RU (resonance units), with 1 RU corresponding to ~1pg protein mm^{-2} (50, 105). It is recorded at a time resolution up to ~0.1 s. In the terminology of the SPR biosensor literature, a binding-progress curve is called a sensorgram.

The most frequently used commercial SPR instruments (BIAcore) place the sensor surface on a removable microchip that is optically coupled to the instrument; the sample is supplied via an integrated computer-controlled microfluidic system (103) [flow-cell dimensions 2.1 mm × 0.55 mm × 0.05 mm (l × w × h) with a detection area of 0.2 mm^2 (44)]. The commercial resonant mirror device is based on a cuvette system that is equipped with a vibro-stirrer (116).

SENSOR SURFACES AND IMMOBILIZATION

Although SPR biosensors do not require the labeling of reactants, one of the binding partners has to be immobilized on the sensor surface (which may be regarded as an equivalent to a label of macroscopic size). For the analysis of binding affinities and kinetics it is crucial that the measured binding reflects exclusively the native interaction of both reactants, i.e. that nonspecific surface-binding is negligible and that the immobilization does not affect the conformation of the binding site. Preferably, the macromolecule should be attached with uniform orientation and unrestrained accessibility for the mobile reactant. The sensor surface and the immobilization technique employed are therefore very important, and a number of different techniques have been described. Obviously, the best choice of which binding partner to immobilize and which immobilization technique to employ depends on the particular set of interacting macromolecules; if possible, the comparative use of different techniques seems to be advantageous (17, 68, 83, 110).

The gold surface on the SPR sensor chip is usually covered with a self-assembled monolayer of alkyl thiols. This suppresses nonspecific binding and creates a hydrophilic surface (58). In most of the biosensor applications, sensor chips are used in which a matrix of carboxymethylated dextran is covalently attached (1–3 ng/mm^2) (58) to form a flexible hydrogel of estimated thickness 100–200 nm (105) or 200–400 nm (116). As is the case with chromatographic matrices, this dextran matrix can be derivatized to give a number of different functional groups and to allow for a variety of immobilization chemistries (see below) (13, 26, 43, 76, 104). A regeneration procedure for this sensor chip has been described (10). The particular advantage of using this flexible, hydrophilic dextran matrix is that it provides better accessibility of the immobilized macromolecules to their binding partners, and a potentially

increased signal from the SPR sensor, by virtue of a relatively large number of immobilized binding sites and more efficient use of the evanescent field (58, 59).

A widely applied immobilization procedure utilizes activation of the carboxy groups of the dextran gel with a mixture of *N*-hydroxysuccinimide (NHS) and *N*-ethyl-*N′* (dimethylaminopropyl) carbodiimide to form NHS esters, which enables coupling to the amino groups on proteins (42). The effectiveness of the coupling relies on a preconcentration of the protein by electrostatic attraction to the negatively charged matrix at pH values below the pI of the protein (42, 58). However, it has been noted that this may lead to protein denaturation (68, 104). Another disadvantage of the NHS-ester immobilization procedure is the potential occurrence of random coupling to different lysines on the protein (76), which may introduce subpopulations of binding sites with different accessibilities and reactivities.

For these reasons, a variety of more specific immobilization methods have been described (43, 76), such as coupling by thiol/disulfide exchange (13, 43), aldehyde coupling (43), hydrazide group coupling (76), sulfhydryl group coupling (53, 76), and chelate linkage of oligohistidine tags (26, 78, 101). In several studies, for example, a specific orientation of the immobilized receptor domain was achieved by creating a thiol coupling/disulfide bond to cysteine residues that were introduced into one reactant via site-directed mutagenesis (13, 86, 100). For the immobilization of proteins with hydrophobic anchors, modification of the dextran matrix by heptyl residues has been described (104). Covalent linkage could be achieved through a perfluorophenylazide-derived hydrophobic crosslinker (104).

Indirect coupling, exploiting the high affinity of the avidin-biotin interaction, can be achieved by immobilizing avidin/streptavidin to the dextran matrix and binding biotinylated macromolecules (4, 43, 45, 76). This method has the additional advantage of not requiring preconcentration in the matrix. It has been preferred for the immobilization of DNA and RNA (5, 7, 45) but has also been generally used, for example, to immobilize lipid vesicles (66). A related technique is the use of a sandwich assay, in which an antibody that can specifically capture one of the reactants is immobilized (49, 83).

Since the presence of the flexible, negatively charged dextran gel [allowing for nonspecific electrostatic adsorption (35, 58, 117)] combined with high immobilization densities may interfere with the requirements for a kinetic analysis (see below), the use of a planar sensor surface can be advantageous (17, 84, 97). Novel methods of immobilization have been and are being developed. The immobilization on aminosilane-derivatized surfaces (employing a resonant mirror biosensor) has been described (8, 17). Alternatively, the use of mixed self-assembled monolayers of functionalized alkyl thiols on the gold surface of

the SPR biosensor has been demonstrated (16, 70, 101, 108) and reviewed (71). Different methods to construct supported bilayers can be employed (36, 84, 88, 92, 93). Ramsden et al used the Langmuir-Blodgett and Langmuir-Schaefer method to deposit lipid bilayers onto the surface of the grating coupler instrument (88), while Plant et al employed phospholipid vesicle fusion on a self-assembled alkanethiol monolayer to construct a supported hybrid bilayer on the sensor chip of the SPR instrument (84).

After successful immobilization of one of the reactants to the sensor surface, the real-time detection of local changes in the refractive index at the sensor surface upon introduction of reactants into the mobile phase is a versatile tool for the study of reversible interactions. The following discussion is confined to the quantitative analysis of binding equilibria and kinetics.

DATA ANALYSIS

A Simple Model for a Biomolecular Interaction

In the simplest model for the interaction of an immobilized species X (for example a receptor) and a mobile macromolecule L (a ligand), both reactants reversibly form a 1:1 complex XL, at a chemical on–rate constant for complex formation k_+, and a chemical off–rate constant for complex dissociation k_-. The thermodynamic equilibrium dissociation constant is then equal to

$$K_D = k_-/k_+. \tag{1}$$

Under ideal conditions, neglecting all potential complications due to the finite volume in which the reaction takes place, and assuming that the concentration of the mobile reactant is held constant by an infinitely fast exchange with the bulk solution, the pseudo-first-order rate equation

$$\mathrm{d[XL]/dt} = k_+[\mathrm{L}]([\mathrm{X}]_{\mathrm{tot}} - [\mathrm{XL}]) - k_-[\mathrm{XL}] \tag{2}$$

is valid, where [L] is constant and $[\mathrm{X}]_{\mathrm{tot}}$ denotes the total binding capacity of the surface on a molar basis. Usually, in an SPR biosensor experiment, relatively high concentrations of immobilized binding sites are required to produce a significant refractive index change upon binding. Therefore, the signal contribution of the free mobile reactant can usually be neglected. With the biosensor response R proportional to [XL], Equation 2 gives

$$\mathrm{dR/dt} = k_+\mathrm{f}_0\mathrm{R}_{\mathrm{sat}} - (k_+\mathrm{f}_0 + k_-)\mathrm{R}, \tag{3}$$

where $\mathrm{f}_0 \equiv [\mathrm{L}]$, and $\mathrm{R}_{\mathrm{sat}}$ denotes the response at complete saturation of the immobilized binding sites.

If no mobile reactant has been initially bound, the time-course of binding is described by an exponential

$$R(t) = R_{eq}(f_0)[1 - \exp(-k_{obs}t)], \quad (4)$$

with the observed rate constant

$$k_{obs} = k_+ f_0 + k_-, \quad (5)$$

approaching the equilibrium plateau signal

$$R_{eq}(f_0) = R_{max}\left[1 + k_-/(k_+ f_0)\right]^{-1} = R_{max}\left[1 + K_D/f_0\right]^{-1} \quad (6)$$

(Figure 1). Equation 6 is equivalent to a Langmuir isotherm (57). [An expression for the binding isotherm for multivalent binding-species L has been given (46)]. If the free mobile reactant is removed from the buffer ($f_0 = 0$ for $t > t_0$), the complex dissociates exponentially with time:

$$R(t) = R(t_0)\exp[-k_-(t - t_0)]. \quad (7)$$

It should be noted that in this model the observed binding rate constant k_{obs} in the association phase is always higher than the chemical off–rate constant k_-.

Determination of Equilibrium Constants

The thermodynamic equilibrium constant can be determined by the analysis of the dependence of the equilibrium plateau signals on the concentration of free mobile reactant using Equation 6 (for example in a Scatchard analysis), or via measurement of the kinetic rate constants (see below) and using Equation 1 (49).

A very important advantage of the thermodynamic approach is that it does not require modeling of the binding progress (113) and therefore is independent of mass transport influences. In the cuvette-based biosensor systems, equilibrium experiments may be performed employing a stepwise equilibrium titration procedure (34). The thermodynamic approach can also be applied for reactions that are too fast for a kinetic analysis (56). On the other hand, especially for slow reactions and small concentrations of mobile reactant, it may not be possible to reach equilibrium within the frequently limited time frame of an association experiment (6, 33, 75, 113). In this case, the equilibrium analysis cannot be applied; however, the equilibrium response may be extrapolated on the basis of assumptions about the binding kinetics (79). Also, accurate determination of the equilibrium response can suffer from a signal offset due to a refractive index mismatch as a result of the buffer change and a corresponding baseline offset ("bulk effect") or a baseline drift that might be caused by, for example, small temperature variations (25, 51) or nonspecific binding. However, this problem can be addressed using multiple flow cells and comparing the signal to that

obtained in the absence of immobilized reactant (51). This can be particularly useful in the study of weak interactions (6, 61, 109), such as the binding of cell-adhesion molecules (109).

In another experimental variant, free species X over a range of concentrations is pre-equilibrated with reactant L in the mobile phase, and the effects on the equilibrium response (67, 113), or on the binding rate constant k_{obs} of L to the sensor surface (48, 73, 79), are monitored. Although the SPR biosensor measures surface binding, these competition experiments indirectly allow for the determination of the affinity of X and L in solution. This enables diagnosis of the effects of immobilization (73, 113). Also, such competitive experiments facilitate the detection of interactions with small reactants that would give an inadequate response in a direct SPR experiment (47, 48). The kinetic variant of the competition analysis similarly can avoid problems resulting from mass transport and other factors confounding the interpretation of binding kinetics, if the binding rate constants k_{obs} are purely operationally defined. This approach can rely solely on their linear dependency on the concentration of free reactant L (47, 73, 79) or, alternatively, a plot of the empirical dependence of $k_{obs}([L])$ may serve as a calibration for the determination of the concentration of free reactant L (34). This variant of the competition experiment does not require the attainment of binding equilibrium.

Analysis of Binding Kinetics

The analysis of the kinetics of the interaction requires mathematical modeling of the binding-progress curves. For the simple 1:1 interaction, the pseudo-first-order kinetics exhibits a single exponential approach to the equilibrium signal (Equations 4 and 7).

Two different data analysis strategies have been proposed to extract the rate constants k_{obs} and k_-: linear regression of plots of dR/dt vs R for the association phase and $\ln[R(t_0)/R(t)]$ vs time for the dissociation phase (49); alternatively, a nonlinear fit with the integrated rate equations (Equations 4–7) may be used (77). Although equivalent in principle, except for the more advantageous error distributions in the nonlinear regression (77), these strategies differ in their potential for ease of extension to account for the influence of mass transport (49, 98), or for the presence of different subpopulations of binding sites (77), respectively. A fit of Equation 5 to $k_{obs}(f_0)$ obtained in a series of experiments at different concentrations of mobile reactant reveals both chemical rate constants k_+ and k_- (49). In practice, however, k_- may be poorly defined by this method, and therefore the analysis of the dissociation phase is advantageous (49, 77). To account for artifacts of refractive index mismatch during the buffer change, the initial parts of the association and dissociation phases are usually excluded from the analysis (77). In combination with this adjustment, when

nonlinear regression is used, a parameter for an unknown baseline, which in some studies may include baseline drift (4, 7, 47), is added to Equations 4 and 7.

Since the experimental binding-progress curves often do not follow a single exponential (see below) and can be best fit with double exponential expressions, the use of a model with two independent classes of immobilized binding sites has been proposed (77). This model allows for fitting the data with equations similar to Equations 4 and 7 but extended to a superposition of independent terms for each binding site (17, 77). Similarly, a model for the interaction of two different mobile reactants competing for one class of immobilized binding sites leads to double exponential expressions, and has been proposed for use in kinetic competition experiments (47).

Many bimolecular interactions might not follow simple pseudo-first-order binding kinetics. For example, isomerism of antibodies and equilibria between different conformations having different kinetic properties has been suggested to be a widespread phenomenon (23). In this case, the binding-progress curves have to be modeled with more complex rate equations (50, 69). These analyses could, in principle, be performed by global analysis of data from a series of experiments obtained under a variety of different concentrations of mobile and immobile reactants (21, 28, 69). However, the practical limitations of the biosensor experiments appear to severely constrain this approach (28, 97). It has been pointed out that mass transport limitation and related inhomogeneities within the sensor can appear as artifacts in the measured binding-progress curves, and that these can be similar to the results expected from more complicated binding schemes, such as apparently cooperative binding and multi-exponential binding (see below) (97). Nevertheless, at least some qualitative information about more complex binding schemes may be obtained. For example in a study by Glaser & Hausdorf (28), a number of different experiments qualitatively suggested the presence of a slow conformational change of one reactant.

EXPERIMENTAL RESULTS

Comparison with the Theory and with Results Obtained by Other Techniques

Equilibrium measurements have generally yielded data that conform with Equation 6. In some studies, the extracted equilibrium constant was shown to be independent of both the coupling chemistry and the choice of the binding partner that was immobilized (110). Similarly, binding-progress curves obeying Equations 4 and 7 have been found frequently. However, in most studies, the kinetics of binding deviated from the expected single-exponential association and dissociation process (21, 50, 69, 79). Instead, apparently multi-exponential

or sigmoid binding progress of the association phase was observed; in the dissociation phase, double exponential curves are very common. Although this can be an indication of multi-step binding mechanisms or an effect of multi-valency, these shapes were also observed for systems that were expected to follow simple pseudo-first-order kinetics. Therefore, these deviations were frequently attributed to the presence of subpopulations of immobilized binding sites (either intrinsically present or produced by nonuniform immobilization), to the effects of steric hindrance at the sensor surface, or to artifacts resulting from mass transport limitation, which for the dissociation phase are also referred to as rebinding.

Nevertheless, in most published studies it has been argued that Equations 4 and 7, for pure pseudo-first-order binding, would be valid for an appropriately selected data subset. It has been noted that this approach can lead to arbitrary and internally inconsistent results (75, 99), such as, for example, ratios of k_-/k_+ that are different by orders of magnitude from the equilibrium constant K_D as derived from the equilibrium plateau signals, thus violating Equation 1; negative extrapolated values of k_{obs} at $f_0 = 0$; or observed binding rate constants in the association phase k_{obs} smaller than k_-, thus violating Equation 5 (99). It has been advocated that the derived kinetic rate constants should be interpreted as "apparent" rate constants (50). However, it has been pointed out that for data that clearly do not conform to the model on which the derivation of the rate constants is based, the use of such rate constants can be questioned (4, 75, 99).

Many studies have compared the results of biosensor experiments with equilibrium constants and kinetic rate constants obtained for the same interacting macromolecule system by biosensor experiments in other laboratories (38, 56, 116), as well as with different methods, such as calorimetry (4, 17, 41, 56, 62), sedimentation equilibrium (31, 63), fluorescence quenching (9, 40), ELISA (32, 73), and filter binding assays (106). In some cases, good agreement was found within the limits of experimental uncertainty (41, 62, 114, 116). In other studies, however, significant differences were apparent (4, 9, 31, 38, 40, 106, 116), including differences of up to several orders of magnitude (5, 32). Nieba and associates found that even the relative affinities of antibodies for different haptens can be significantly different in kinetic biosensor experiments when compared to ELISA competition experiments (73).

While it is obviously impossible to find general explanations, these observed inconsistencies and discrepancies underline the importance of rigorous data analyses and control experiments. Supporting this view is the finding of Ladbury et al (56) that differences between the results obtained with SPR and those obtained with calorimetry were resolved if appropriate controls were adopted. Similarly, by changing the approach from an analysis of the binding kinetics to a competition experiment for the determination of the equilibrium

constants, Nieba et al (73) were able to resolve the inconsistencies with the result from ELISA experiments. In the following discussion, some possible sources of artifacts in SPR biosensor experiments together with proposed diagnostic and data analysis techniques are described.

Possible Effects of the Immobilization

Obviously, the immobilization of reactants to the sensor surface can in some cases interfere with their binding properties by, for example, inducing conformational changes in the binding sites or sterically restricting the access of the binding partner. If a nonspecific immobilization chemistry such as amine coupling is employed, multiple subpopulations of different orientations and different affinities could be produced (75). This should result in a broadening of the binding isotherm in the equilibrium data, while the binding kinetics could be characterized by multi-exponential binding-progress curves, each exponential term reflecting binding to a subpopulation of independent binding sites (79).

Based on the empirical observation that single-exponential binding progress is often preserved at low concentrations of the mobile reactant, O'Shannessy & Winzor (79) proposed restriction of the data analysis to those data that are in conformity with the description of simple 1:1 pseudo-first-order kinetics. These data contain the most information on the best accessible binding sites, which can be assumed to best mimic the affinity in solution. Significant binding to more restricted orientations of binding sites with correspondingly lower affinities takes place only at higher concentrations of mobile reactant. On the other hand, apparently multi-exponential binding can also be a result of mass transport limitations and nonuniform distribution of the binding sites within the immobilization matrix (97). In this case, the experiments with low concentrations of mobile reactant would give kinetic curves that appear to be single-exponential, apparently in conformity with pure pseudo-first-order binding (27, 97). However, the rate constants derived from these data could be orders of magnitude below the true intrinsic chemical rate constants (97, 98). Therefore, this ambiguity of the interpretation should be resolved experimentally, by means of control experiments for mass transport limitations (see below) and for artifacts of immobilization. A different choice in the employed coupling chemistry, solution competition experiments, and the complete characterization of the binding isotherm by equilibrium experiments could be potentially useful tools.

Another possible effect of the immobilization that is related to the high surface density of binding sites in biosensor experiments is that some immobilized macromolecules may have the potential for oligomerization (86). If binding properties change with the oligomeric state, or if the mobile reactant is multivalent (56, 86), the results of a biosensor experiment may depend on the surface density of the immobilized species.

Steric Hindrance

It has been noted that high local concentrations of immobilized reactant at the sensor surface can lead to steric hindrance in binding to neighboring binding sites (4, 17, 79, 97). In several studies, high macromolecular concentrations of up to 100 mg/ml and more within the immobilization matrix (97) would make steric hindrance and excluded-volume effects more than likely (118). In some respects, this would affect the binding process in a way similar to that of subclasses of differently accessible binding sites. Both lead to a broadening of the binding isotherm and have the smallest impact on the binding kinetics at low saturation of the binding sites. However, the measured dissociation rate can be expected to be less affected for the excluded-volume effect.

Edwards et al (17) compared the binding kinetics of human serum albumin to an antibody immobilized either in a dextran matrix or on an aminosilane surface. In the presence of the immobilization matrix, the data were well described by a double exponential, while the binding to the aminosilane-bound binding sites was described by a single exponential. Concluding that steric hindrance affected binding within the dextran matrix, the investigators interpreted the fast component of the binding progress as representative of binding events similar to those in solution; they interpreted the slow component as produced by artifacts of steric hindrance or restricted access to the binding sites. With the fast component identified as k_{obs} in Equation 5, a conventional analysis could be performed (17). However, high macromolecule concentrations also reduce the transport of the mobile reactant, and under transport limited conditions, it is the earlier part, and consequently the fast component, of the binding progress that is most influenced by a number of parameters not related to chemical reaction rates (98).

Therefore, again, experimental approaches seem to be superior to the analytical approach. A change in the density of immobilized binding sites can diagnose and eliminate the effects of steric hindrance. It should be noted that the direct attachment to a planar surface in the absence of an immobilization matrix alone does not necessarily eliminate these problems, since the effects of excluded area might persist at high surface densities.

Mass Transport Limitations

For kinetic biosensor experiments, the potential limitation of the binding kinetics by the rate of transport of the mobile reactant to the sensor surface represents an intrinsic problem, since an insufficient transport rate will make it impossible to obtain meaningful information on the chemical kinetics. Interactions of biological macromolecules can be very fast: The on–rate constant for average proteins without long-range attractive or repulsive forces has been predicted to be on the order of 10^6 $M^{-1}sec^{-1}$ (74), and for some interactions, rate constants

several orders of magnitude higher have been measured (24, 91). On the other hand, the upper limit of detectable rate constants for the SPR biosensor may be in the order of 10^6 $M^{-1}sec^{-1}$ (assuming a saturation response of approximately 1000 RU) (33, 44, 50, 79, 97, 116). It has been pointed out that this limit depends on the particular mobile reactant (50, 97) and is very difficult to predict, and that mass transport may start to influence the binding-progress curves at chemical rate constants that are a factor of 10–100 below the transport limit (97). This illustrates the importance of appropriate diagnostic tools and control experiments, and therefore mass transport effects are discussed in some detail here.

In comparison with binding to uniformly distributed reactants in solution, the following additional steps of transport have to be accomplished in the biosensor experiment (Figure 3): (*a*) macroscopic transport through the microfluidic system and across the sensor surface, a process that has been examined at different levels of detail (27, 33, 110); (*b*) diffusion through the nonstirred layer over the surface (27, 50, 97); (*c*) diffusion through the array of binding sites within the immobilization matrix (if such a matrix is used) (97). (A related

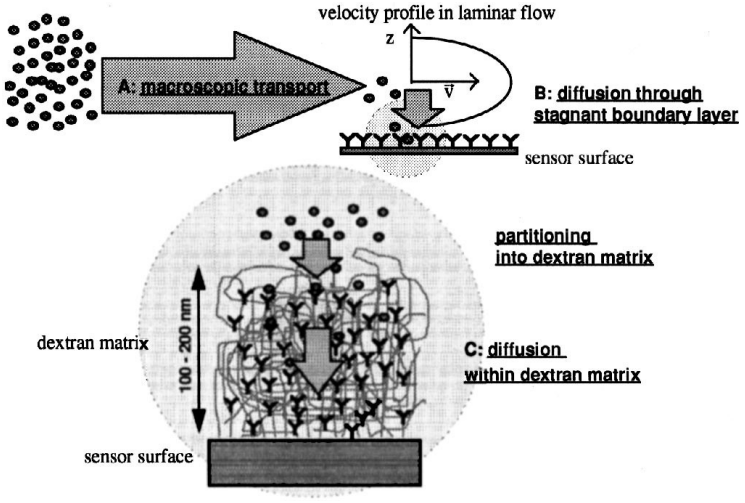

Figure 3 Schematic view of different factors determining transport of the mobile reactant (O) to the sensor surface with immobilized reactant (**Y**): (*a*) macroscopic transport through the microfluidic system (dependent on bulk flow rate); (*b*) diffusion through the nonstirred boundary layer (dependent on bulk flow rate, flow cell geometry, and diffusion coefficient of reactant in bulk solution). Partitioning reduces the concentration of mobile reactant within the dextran matrix; (*c*) diffusion through the immobilization matrix (dependent on size and charge of the reactant, thickness and density of the dextran matrix, and the diffusion coefficient of the reactant in polymer solution).

factor that additionally reduces the collision frequency of the reactants may be the constraints in the translational and rotational diffusion of the immobilized reaction partner (96). All these steps can affect the binding kinetics and lead to transport-controlled binding for reactions that may be far from diffusion control in solution. If not accounted for, this can lead to qualitatively wrong conclusions.

In general, the effects of mass transport–limited binding kinetics to the sensor surface are similar to the transport effects on binding kinetics to cell membranes, which have drawn much theoretical attention (15, 29). Conceptually, in both the association and the dissociation phase, mass transport limitation can be regarded as the failure to maintain the bulk concentration f_0 of the free mobile reactant at the sensor surface in the vicinity of the binding sites (33). To describe it qualitatively, the association phase of a fast surface-binding reaction is characterized by competition of the immobilized binding sites for a limited supply of binding partner and by a local depletion of mobile reactant near the surface. In this case, the replenishment is limited by the transport rate, and the measured binding-progress curve can deviate from an exponential shape (Equation 4) (49, 97). In the dissociation phase, if the rate of dissociation is higher than the transport rate, a nonvanishing concentration of mobile reactant in the vicinity of the sensor surface allows rebinding to empty binding sites (20, 111). This retention effect results in a slower overall dissociation from the surface (102) and can lead to a departure from a single exponential dissociation process.

To approximate these effects quantitatively, a compartment model has been used in a number of studies (22, 27, 72, 97, 98). It assumes a homogeneous distribution of mobile reactant within a bulk compartment and within a compartment at the sensor surface and describes the transport by a single phenomenological transport rate constant k_{tr}. Under steady-state conditions, transport influence on the binding kinetics can be approximated by introducing apparent-reaction rate constants k_+^{app} and k_-^{app}, obeying

$$k_+^{\mathrm{app}}/k_+ = k_-^{\mathrm{app}}/k_- = \left[1 + k_+(\mathrm{R_{sat}} - \mathrm{R})/k_{tr}\right]^{-1} \quad (8)$$

(3, 15, 27, 29, 97, 98). Although this model is a highly simplified description of the coupled binding and transport processes, it provides the important insight that mass transport affects the measured binding progress roughly to the same extent in both the association and the dissociation phases (27, 33, 97), and that it scales directly with the binding capacity of the sensor surface (27, 33, 50, 97).

More information has been obtained by detailed computer simulations of the reaction-diffusion process in the SPR biosensor, which take into account the spatial distribution of the reactants. By this method, the convection/diffusion/surface-binding process in the bulk flow across the sensor surface has been modeled

(27). In another study, the effects of the finite thickness of the immobilization matrix combined with the exponentially decaying sensitivity with increasing distance from the sensor surface, caused by the evanescent wave, were investigated (97). Although this immobilization matrix is only 100–400 nm thick (59, 116), for large reactants the transport within the dextran matrix can be the rate-limiting step in the overall binding. This is mainly caused by the high concentration of the binding sites, partitioning of the mobile reactant from the bulk phase into the matrix, and hindered diffusion through the matrix polymer chains.

Under mass transport–limited conditions, binding in the association phase may be characterized by high spatial inhomogeneities and moving-front phenomena within the sensor. Because of the inhomogeneous detection, which exponentially amplifies the contribution of bound material nearer to the sensor surface, the signal can be affected by these inhomogeneities. In this case, the measured binding-progress curve is governed by factors unrelated to the chemical reaction rates, e.g. diffusion coefficients, partition coefficients, size and charge of the mobile species, distribution of immobilized binding sites, thickness of the dextran matrix, decay length of the evanescent wave, and buffer flow rate. In the dissociation phase, lower spatial inhomogeneities were found (97). If the dissociation phase is started before binding equilibrium has been established, as is often imposed by constraints in the observation time of the association phase, additional artifacts may be introduced, such as a still-increasing signal during the dissociation process (97).

The calculated binding-progress curves in both computer models could nevertheless be empirically fitted by a single exponential similar to Equations 4 and 7 if the concentration of the mobile reactant was lower than the dissociation equilibrium constant. However, the derived rate constants were smaller than the intrinsic chemical rate constants, following Equation 8 (27, 97). At higher concentrations, deviations from exponential binding progress were found. In the association phase, mass transport limitations can result in an initial linear phase, in sigmoidal shapes, and in biphasic, apparently double exponential sensorgrams (27, 49, 97). The dissociation phase can always be empirically well described by a double exponential (97). However, the apparent rate constants derived by an empirical exponential analysis are lower than the intrinsic chemical rate constants.

The data analysis strategy initially proposed to eliminate mass transport influence consisted of the restriction to the analysis of quasi-linear data subsets near the binding equilibrium, for which the validity of Equations 4, 5, and 7 was assumed. Limiting slopes were taken in plots of dR/dt vs R for the association phase, and in plots of $\ln[R(t_0)/R(t)]$ vs time for the dissociation phase to extract k_{obs} and k_- (49, 90, 111). In addition to this, the linearity of these data

transforms was used as a diagnostic tool for the presence of transport limitation. As can be seen from Equation 8, mass transport influences are smaller at low concentrations of empty binding sites (at small differences R_{sat}-R). However, Glaser (27) showed by computer simulations of the mass transport processes above the sensor surface that this method is not successful in extracting reliable chemical rate constants. Unfortunately, this finding has not been appreciated in most of the biosensor literature. However, the invalidity of this approach has been confirmed recently both by computer simulations of the transport within the dextran matrix of the sensor surface, and on theoretical grounds (98). It leads to apparent chemical on–rate constants lying between a totally transport-limited rate constant and the true chemical on–rate constant, depending on the concentrations of mobile reactant used in the experiments.

Global fitting with models including compartment mass transport description terms was proposed by some authors as a tool to analyze transport-influenced data (22, 72). However, it has been pointed out that this does not account for the spatial inhomogeneities caused by the coupled reaction-diffusion process that may govern the binding progress in the association phases at high mass transport influence, simulating apparently complex binding schemes (97). To resolve this difficulty, it has been advocated that the compartment model be restricted to the approach to equilibrium in the association phase and to the dissociation phase, where the spatial inhomogeneities are small (98). Based on this, the approximate expressions were proposed for mass transport-influenced binding

$$k_{obs}^{\lim}(\mathrm{f_0}) = (k_+ \cdot \mathrm{f_0} + k_-)/\left[1 + \left(k_+ \mathrm{R_{sat}}/k_{tr}\right)\left(1 + k_+ \mathrm{f_0}/k_-\right)^{-1}\right] \quad (9)$$

in the association phase, and

$$\mathrm{dR/dt} = -k_- \mathrm{R}/\left[1 + k_+(\mathrm{R_{sat}} - \mathrm{R})/k_{tr}\right]. \quad (10)$$

in the dissociation phase. Here $k_{obs}^{\lim}$ is evaluated only in the limit of the approach to equilibrium, and k_{tr} denotes a phenomenological transport rate constant (98), replacing Equations 5 and 7 as fitting equations. These expressions realistically have the property to yield only lower limits for chemical reaction rate constants for mass transport-controlled binding. Equation 10 describes the dissociation/rebinding process and may be used to distinguish multiphasic binding caused by reaction schemes more complicated than the 1:1 interaction from apparent double exponential dissociation caused by rebinding (98).

By far the best approach to mass transport problems, however, involves a change of the experimental setup, especially in the presence of more complex binding schemes. The use of the lowest possible binding capacity has been recommended to minimize transport effects, which represents a trade-off against a high signal/noise ratio (27, 33, 50, 97). Furthermore, a variation of the binding

capacity in experiments with different surfaces can be used as a tool to show the absence of mass transport influence on the derived kinetic parameters (27, 28, 50). Also, experiments done at concentrations of the mobile reactant in a range from approximately tenfold smaller to tenfold higher than the equilibrium dissociation constant are desirable to diagnose the extent of mass transport limitation. Provided that the required amount of material is available, these control experiments are relatively easy to perform, considering the high degree of automation available and the possible use of several flow channels in parallel (51).

Another test for mass transport influence that has often been applied is the variation of the buffer flow rate (9, 19, 27, 49), which modulates the rate of replenishment or wash-out of mobile reactant above the sensor surface. While a change in the buffer flow directly changes the macroscopic transport linearly (110), this method has two major disadvantages concerning the microscopic steps of the transport. First, the diffusion through the nonstirred layer is determined only by the cube root of the flow speed (27, 60). Second, if an immobilization matrix is used, diffusion through this matrix will not be affected by the buffer flow rate, although it may represent the rate limiting step of the transport (97). It appears that it might be more advantageous to test for mass transport influence by changing the buffer viscosity, for example by the addition of sucrose or glycerol (3, 98).

Finally, an elegant way to reduce mass transport influence is the addition of a binding competitor to the dissociation buffer (for example a soluble derivative of the immobilized reactant) (15, 20, 27, 80, 90, 97, 106). If the competitor can be transported fast enough to the sensor surface and penetrates the immobilization matrix (97), it can block the empty binding sites, preventing rebinding and therefore accelerating the transport of the mobile reactant. Unfortunately, this technique can only eliminate mass transport influences in the dissociation phase, while they persist in the association phase. However, this technique can be combined with an equilibrium analysis to derive the on–rate constants via the identity $k_+ = k_-/K_D$ (20).

CONCLUSIONS AND FUTURE PERSPECTIVES

The use of SPR and related biosensors to characterize reversible macromolecular interactions is a young technique that has been successfully employed in many studies. On the other hand, with an increasing number of applications available for the quantitative determination of equilibrium and kinetic rate constants, several critical potential artifacts have been identified.

In addition to the problems of mass transport, immobilization in multiple conformations, steric hindrance, the use of data subset analysis, and the lack of self-consistency, as described above, caution was also advocated for the influence of

multimeric aggregates of mobile reactants (56, 62, 109), the inappropriate use of a simple 1:1 pseudo-first-order description for binding of multivalent mobile reactants (46, 62, 73), and for the lack of replicates and statistical analysis (75). In retrospect, in the absence of appropriate control experiments or analytical approaches, the validity of some or even most of the published kinetic rate and equilibrium constants has been questioned (21, 56, 62, 73, 75, 79, 97–99, 109).

At the same time, a number of different immobilization chemistries, experimental controls for potential artifacts, and analytical techniques have been developed. Combined, they should allow for a rigorous measurement of kinetic rate and equilibrium constants, or they should at least unambiguously identify sources of deviations from the expected binding-progress curves and binding isotherms. Unfortunately, the analyses of the effects of heterogeneity of binding sites or excluded volume and the effects of mass transport limitation lead to contradictory results in that they conclude that different parts of the binding-progress curves contain critical information on the chemical binding reaction. In addition, because of their complexity these effects cannot be modeled by global analysis approaches (79, 98). Consequently, experimental controls seem indispensable, even regardless of the possible apparent conformity of the measured binding-progress curves with a simple 1:1 model. For example, the use of several different densities of immobilized reactant can diagnose and simultaneously minimize influences of mass transport and steric hindrance/excluded volume. However, the relative difference of the binding capacities should be much higher than the relative statistical error in the derived rate constants. Likewise, apparent heterogeneity of the binding sites should, if possible, be experimentally verified, for example, by a change of the coupling chemistry or by solution competition experiments. If these and other confounding factors can be excluded on the basis of control experiments, global analysis approaches can be helpful to ensure internally consistent data analyses, and can eventually indicate more complex reaction schemes. But, even if it is not possible to resolve kinetic rate constants, in the biological context, information on the lower limits of the rate constants might itself be valuable.

A particularly interesting area of development is the use of planar sensor surfaces with proteins, such as membrane-bound receptors, incorporated into supported bilayers (36, 84, 88, 94). This configuration provides lateral mobility of the receptor in the bilayer and could serve as a model for the interaction of macromolecules in the mobile phase with biomembranes (92).

In summary, it appears that the necessary tools for the reliable determination of reaction rate and equilibrium constants with optical evanescent wave biosensors are available. However, the need for critical awareness of the potential pitfalls of the method has been emphasized by several authors (33, 73, 75, 79, 97, 99, 109).

ACKNOWLEDGMENTS

I am grateful to Marc Lewis, David Margulies, Peter McPhie, David Millar, Allen Minton, and Daniel O'Shannessy for stimulating discussions and comprehensive help on improving the manuscript. I thank especially Marc Lewis and Allen Minton for their continuous support.

Literature Cited

1. Alam SM, Travers PJ, Wung JL, Nasholds W, Redpath S, et al. 1996. T-cell-receptor affinity and thymocyte positive selection. *Nature* 381:616–20
2. Bates PJ, Dosanjh HS, Kumar S, Jenkins TC, Laughton CA, et al. 1995. Detection and kinetic studies of triplex formation by oligodeoxynucleotides using real-time biomolecular interaction analysis (BIA). *Nucleic Acids Res.* 23:3627–32
3. Berg OG, von Hippel PH. 1985. Diffusion-controlled macromolecular interactions. *Annu. Rev. Biophys. Biophys. Chem.* 14:131–60
4. Bernard A, Bosshard HR. 1995. Real-time monitoring of antigen-antibody recognition on a metal oxide surface by an optical grating coupler sensor. *Eur. J. Biochem.* 230:416–23
5. Bondeson K, Frostell-Karlsson Å, Fägerstam L, Magnusson G. 1993. Lactose repressor-operator DNA interactions: kinetic analysis by a surface plasmon resonance biosensor. *Anal. Biochem.* 214:245–51
6. Boniface JJ, Davis MM. 1994. The kinetics of binding of peptide/MHC complexes to T-cell receptors: application of surface plasmon resonance to a low-affinity measurement. *Methods Enzymol.* 6:168–76
7. Buckle M, Williams RM, Negroni M, Buc H. 1996. Real time measurements of elongation by a reverse transcriptase using surface plasmon resonance. *Proc. Natl. Acad. Sci. USA* 93:889–94
8. Buckle PE, Davies RJ, Kinning T, Yeung D, Edwards PR, et al. 1993. The resonant mirror: a novel optical sensor for direct sensing of biomolecular interactions. Part II: Applications. *Biosensors Bioelectron.* 8:355–63
9. Chaiken I, Rosé S, Karlsson R. 1992. Analysis of macromolecular interactions using immobilized ligands. *Anal. Biochem.* 201:197–210
10. Chatelier RC, Gengenbach TR, Griesser HJ, Brigham-Burke M, O'Shannessy DJ. 1995. A general method to recondition and reuse BIAcore sensor chips fouled with covalently immobilized protein/peptide. *Anal. Biochem.* 229:112–18
11. Chatelier RC, Minton AP. 1996. Adsorption of globular proteins on locally planar surfaces: models for the effect of excluded surface area and aggregation of adsorbed protein on adsorption equilibria. *Biophys. J.* 71:2367–74
12. Corr M, Slanetz AE, Boyd LF, Jelonek MT, Khilko S, et al. 1994. T cell receptor-MHC class I peptide interactions: affinity, kinetics, and specificity. *Science* 265:946–49
13. Cunningham BC, Wells JA. 1993. Comparison of a structural and a functional epitope. *J. Mol. Biol.* 234:554–63
14. Cush R, Cronin JM, Steward WJ, Maule CH, Molloy J, et al. 1993. The resonant mirror: a novel optical biosensor for direct sensing of biomolecular interactions. Part I: Principle of operation and associated instrumentation. *Biosens. Bioelectron.* 8:347–53
15. DeLisi C. 1980. The biophysics of ligand-receptor interactions. *Q. Rev. Biophys.* 13:201–30
16. Duschl C, Sévin-Landais A-F, Vogel H. 1996. Surface engineering: optimization of antigen presentation in self-assembled monolayers. *Biophys. J.* 70:1985–95
17. Edwards PR, Gill A, Pollard-Knight DV, Hoare M, Buckle PE, et al. 1995. Kinetics of protein-protein interactions at the surface of an optical biosensor. *Anal. Biochem.* 231:210–17
18. Fägerstam LG, Frostell Å, Karlsson R, Kullman M, Larsson A, et al. 1990. Detection of antigen-antibody interactions by surface plasmon resonance. Application to epitope mapping. *J. Mol. Recogn.* 3:208–14

19. Fägerstam LG, Frostell-Karlsson Å, Karlsson R, Persson B, Rönnberg I. 1992. Biospecific interaction analysis using surface plasmon resonance detection applied to kinetic, binding site and concentration analysis. *J. Chromatogr.* 597:397–410
20. Felder S, Zhou M, Hu P, Ureña J, Ullrich A, et al. 1993. SH2 domains exhibit high-affinity binding to tyrosine-phosphorylated peptides yet also exhibit rapid dissociation and exchange. *Mol. Cell. Biol.* 13:1449–55
21. Fisher RJ, Fivash M. 1994. Surface plasmon resonance based methods for measuring the kinetics and binding affinities of biomolecular interactions. *Curr. Opin. Biotechnol.* 5:389–95
22. Fisher RJ, Fivash M, Casas-Finet J, Bladen S, McNitt KL. 1994. Real-time BIAcore measurement of *Escherichia coli* single-stranded DNA binding (SSB) protein to polydeoxythymidylic acid reveal single-state kinetics with steric cooperativity. *Methods: Companion Methods Enzymol.* 6:121–33
23. Foote J, Milstein C. 1994. Conformational isomerism and the diversity of antibodies. *Proc. Natl. Acad. Sci. USA* 91:10370–74
24. Foote J, Milstein C. 1991. Kinetic maturation of an immune response. *Nature* 352:530–32
25. Garland PB. 1996. Optical evanescent wave methods for the study of biomolecular interactions. *Q. Rev. Biophys.* 29:91–117
26. Gershon PD, Khilko S. 1995. Stable chelating linkage for reversible immobilization of oligohistidine tagged proteins in the BIAcore surface plasmon resonance detector. *J. Immunol. Methods* 183:65–76
27. Glaser RW. 1993. Antigen-antibody binding and mass transport by convection and diffusion to a surface: A two-dimensional computer model of binding and dissociation kinetics. *Anal. Biochem.* 213:152–61
28. Glaser RW, Hausdorf G. 1996. Binding kinetics of an antibody against HIV p24 core protein measured with real-time biomolecular interaction analysis suggest a slow conformational change in antigen p24. *J. Immunol. Methods* 189:1–14
29. Goldstein B, Dembo M. 1995. Approximating the effects of diffusion on reversible reactions at the cell surface: ligand-receptor kinetics. *Biophys. J.* 68:1222–30
30. Gotoh M, Hasegawa Y, Shinohara Y, Shimizu M, Tosu M. 1995. A new approach to determine the effect of mismatches on kinetic parameters in DNA hybridization using an optical biosensor. *DNA Res.* 2:285–93
31. Gruen LC, Kortt AA, Nice E. 1993. Determination of relative binding affinity of influenza virus N9 sialidases with the Fab fragment of monoclonal antibody NC41 using biosensor technology. *Eur. J. Biochem.* 217:319–25
32. Guichard G, Benkirane N, Zeder-Lutz G, Van Regenmortel MHV, Briand J-P, et al. 1994. Antigenic mimicry of natural L-peptides with retro-inverso-peptidomimetics. *Proc. Natl. Acad. Sci. USA* 91:9765–69
33. Hall DR, Cann JR, Winzor DJ. 1996. Demonstration of an upper limit to the range of association rate constants amenable to study by biosensor technology based on surface plasmon resonance. *Anal. Biochem.* 235:175–84
34. Hall DR, Winzor DJ. 1997. Use of a resonant mirror biosensor to characterize the interaction of carboxypeptidase A with an elicited monoclonal antibody. *Anal. Biochem.* 244:152–60
35. Hemminki A, Hoffrén A-M, Takkinen K, Vehniäinen M, Mäkinen M-L, et al. 1995. Introduction of lysine residues on the light chain constant domain improves the labelling properties of a recombinant Fab fragment. *Protein Eng.* 8:185–91
36. Heyse S, Vogel H, Sänger M, Sigrist H. 1995. Covalent attachment of functionalized lipid bilayers to planar waveguides for measuring protein binding to biomimetic membranes. *Protein Sci.* 4:2532–44
37. Hodgson J. 1994. Light, angles, action. *Bio-Technology* 12:31–35
38. Holliger P, Prospero T, Winter G. 1993. "Diabodies": small bivalent and bispecific antibody fragments. *Proc. Natl. Acad. Sci. USA* 90:6444–48
39. Huber W, Barner R, Fattinger C, Hübscher J, Koller H, et al. 1992. Direct optical immunosensing (sensitivity and selectivity). *Sensors Actuators B* 6:122–26
40. Ito W, Kurosawa Y. 1993. Development of an artificial antibody system with multiple valency using an Fv fragment fused to a fragment of protein *A. J. Biol. Chem.* 268:20668–75
41. Johanson K, Appelbaum E, Doyle M, Hensley P, Zhao B, et al. 1995. Binding interactions of human interleukin 5 with its receptor subunit. *J. Biol. Chem.* 270:9459–71
42. Johnsson B, Löfås S, Lindquist G. 1991. Immobilization of proteins to

a carboxymethyldextran-modified gold surface for biospecific interaction analysis in surface plasmon resonance sensors. *Anal. Biochem.* 198:268–77

43. Johnsson B, Löfås S, Lindquist G, Edström Å, Hillgren R-MM, et al. 1995. Comparison of methods for immobilization to carboxymethyl dextran sensor surfaces by analysis of the specific activity of monoclonal antibodies. *J. Mol. Recogn.* 8:125–31
44. Jönsson U, Malmqvist M. 1992. Real time biospecific interaction analysis. *Adv. Biosensors* 2:291–336
45. Jost J-P, Munch O, Andersson T. 1991. Study of protein-DNA interactions by surface plasmon resonance (real time kinetics). *Nucleic Acids Res.* 19:2788
46. Kalinin NL, Ward LD, Winzor DJ. 1995. Effects of solute multivalence on the evaluation of binding constants by biosensor technology: Studies with concanavalin A and interleukin-6 as partitioning proteins. *Anal. Biochem.* 228:238–44
47. Karlsson R. 1994. Real-time competitive kinetic analysis of interactions between low-molecular-weight ligands in solution and surface-immobilized receptors. *Anal. Biochem.* 221:142–51
48. Karlsson R, Jendeberg L, Nilsson B, Nilsson J, Nygren P-Å. 1995. Direct and competitive kinetic analysis of the interaction between human IgG1 and a one domain analogue of protein A. *J. Immunol. Methods* 183:43–49
49. Karlsson R, Michaelsson A, Mattson L. 1991. Kinetic analysis of monoclonal antibody-antigen interactions with a new biosensor based analytical system. *J. Immunol. Methods* 145:229–40
50. Karlsson R, Roos H, Fägerstam L, Persson B. 1994. Kinetic and concentration analysis using BIA technology. *Methods: Companion Methods Enzymol.* 6:99–110
51. Karlsson R, Ståhlberg R. 1995. Surface plasmon resonance detection and multispot sensing for direct monitoring of interactions involving low-molecular-weight analytes and for determination of low affinities. *Anal. Biochem.* 228:274–80
52. Kelley RF, O'Connell MP. 1993. Thermodynamic analysis of an antibody functional epitope. *Biochemistry* 32:6828–35
53. Khilko SN, Corr M, Boyd LF, Lees A, Inman JK, et al. 1993. Direct detection of major histocompatibility complex class I binding to antigenic peptides using surface plasmon resonance. *J. Biol. Chem.* 268:15425–34
54. Kretschmann E, Raether H. 1968. Radiative decay of non-radiative surface plasmons excited by light. *Z. Naturforsch. Teil A* 23:2135–36
55. Kuziemko GM, Stroh M, Stevens RC. 1996. Cholera toxin binding affinity and specificity for gangliosides determined by surface plasmon resonance. *Biochemistry* 35:6375–84
56. Ladbury JE, Lemmon MA, Zhou M, Green J, Botfield MC, et al. 1995. Measurement of the binding of tyrosyl phosphopeptides to SH2 domains: a reappraisal. *Proc. Natl. Acad. Sci. USA* 92:3199–203
57. Langmuir I. 1918. The adsorption of gases on plane surfaces of glass, mica and platinum. *J. Am. Chem. Soc.* 40:1361–403
58. Löfås S, Johnsson B. 1990. A novel hydrogel matrix on gold surfaces in surface plasmon resonance sensors for fast and efficient covalent immobilization of ligands. *J. Chem. Soc. Chem. Commun.* 21:1526–28
59. Löfås S, Malmqvist M, Rönnberg I, Stenberg E, Liedberg B, et al. 1991. Bioanalysis with surface plasmon resonance. *Sensors Actuators B* 5:79–84
60. Lok BK, Cheng Y-L, Robertson CR. 1983. Protein adsorption on crosslinked polydimethylsiloxane using total internal reflection fluorescence. *J. Colloid Interface Sci.* 91:104–16
61. Lyons DS, Lieberman SA, Hampl J, Boniface JJ, Chien Y-h, et al. 1996. A TCR binds to antagonist ligands with lower affinities and faster dissociation rates than to agonists. *Immunity* 5:53–61
62. MacKenzie CR, Hirama T, Deng S-j, Bundle DR, Narang SA, et al. 1996. Analysis by surface plasmon resonance of the influence of valence on the ligand binding affinity and kinetics of an anti-carbohydrate antibody. *J. Biol. Chem.* 271:1527–33
63. Malchiodi EL, Eisenstein E, Fields BA, Ohlendorf DH, Schlievert PM, et al. 1995. Superantigen binding to a T cell receptor beta chain of known three-dimensional structure. *J. Exp. Med.* 182:1833–45
64. Malmborg AC, Borrebaeck CA. 1995. BIAcore as a tool in antibody engineering. *J. Immunol. Methods* 183:7–13
65. Margulies DH, Plaksin D, Khilko SN, Jelonek MT. 1996. Studying interactions involving the T-cell antigen receptor by surface plasmon resonance. *Curr. Opin. Immunol.* 8:262–70
66. Masson L, Mazza A, Brousseau R. 1994. Stable immobilization of lipid vesicles for kinetic studies using surface plas-

mon resonance. *Anal. Biochem.* 218:405–12
67. Morelock MM, Ingraham RH, Betageri R, Jakes S. 1995. Determination of receptor-ligand kinetic and equilibrium binding constants using surface plasmon resonance: Application to the lck SH2 domain and phosphotyrosyl peptides. *J. Med. Chem.* 38:1309–18
68. Morton TA, Bennett DB, Appelbaum ER, Cusimano DM, Johanson KO, et al. 1994. Analysis of the interaction between human interleukin-5 and the soluble domain of its receptor using a surface plasmon resonance biosensor. *J. Mol. Recogn.* 7:47–55
69. Morton TA, Myszka DG, Chaiken IM. 1995. Interpreting complex binding kinetics from optical biosensors: A comparison of analysis by linearization, the integrated rate equation, and numerical integration. *Anal. Biochem.* 227:176–85
70. Mrksich M, Grunwell JR, Whitesides GM. 1995. Biospecific adsorption of carbonic anhydrase to self-assembled monolayers of alkanethiolates that present benzenesulfonamide groups on gold. *J. Am. Chem. Soc.* 117:12009–10
71. Mrksich M, Whitesides GM. 1996. Using self-assembled monolayers to understand the interactions of man-made surfaces with proteins and cells. *Annu. Rev. Biophys. Biomol. Struct.* 25:55–78
72. Myszka D, Doyle M. 1996. *Robust analysis of a mass transport limited reaction recorded on an optical biosensor*. Presented at Conf. Revers. Assoc. Struct. Mol. Biol., Bethesda
73. Nieba L, Krebber A, Plückthun A. 1996. Competition BIAcore for measuring true affinities: large differences from values determined from binding kinetics. *Anal. Biochem.* 234:155–65
74. Northrup SH, Erickson HP. 1992. Kinetics of protein-protein association explained by Brownian dynamics computer simulation. *Proc. Natl. Acad. Sci. USA* 89:3338–42
75. O'Shannessy DJ. 1994. Determination of kinetic rate and equilibrium binding constants for macromolecular interactions: a critique of the surface plasmon resonance literature. *Curr. Opin. Biotechnol.* 5:65–71
76. O'Shannessy DJ, Brigham-Burke M, Peck K. 1992. Immobilization chemistries suitable for use in the BIAcore surface plasmon resonance detector. *Anal. Biochem.* 205:132–36
77. O'Shannessy DJ, Brigham-Burke M, Soneson KK, Hensley P, Brooks I. 1993. Determination of rate and equilibrium binding constants for macromolecular interactions using surface plasmon resonance: use of nonlinear least squares analysis methods. *Anal. Biochem.* 212:457–68
78. O'Shannessy DJ, O'Donnell KC, Martin J, Brigham-Burke M. 1995. Detection and quantitation of hexa-histidine-tagged recombinant proteins on western blots and by a surface plasmon resonance biosensor technique. *Anal. Biochem.* 229:119–24
79. O'Shannessy DJ, Winzor DJ. 1996. Interpretation of deviations from pseudo-first-order kinetic behavior in the characterization of ligand binding by biosensor technology. *Anal. Biochem.* 236:275–83
80. Panayotou G, Gish G, End P, Truong O, Gout I, et al. 1993. Interactions between SH2 domains and tyrosine-phosphorylated platelet-derived growth factor β-receptor sequences: Analysis of kinetic parameters by a novel biosensor-based approach. *Mol. Cell. Biol.* 13:3567–76
81. Patten PA, Gray NS, Yang PL, Marks CB, Wedemayer GJ, et al. 1996. The immunological evolution of catalysis. *Science* 271:1086–91
82. Payne G, Shoelson SE, Gish GD, Pawson T, Walsh CT. 1993. Kinetics of $p56^{lck}$ and $p60^{src}$ Src homology 2 domain binding to tyrosine-phosphorylated peptides determined by a competition assay or surface plasmon resonance. *Proc. Natl. Acad. Sci. USA* 90:4902–6
83. Pellequer JL, Van Regenmortel MHV. 1993. Measurement of kinetic binding constants of viral antibodies using a new biosensor technology. *J. Immunol. Methods* 166:133–43
84. Plant AL, Brigham-Burke M, Petrella EC, O'Shannessy DJ. 1995. Phospholipid/alkanethiol bilayers for cell-surface receptor studies by surface plasmon resonance. *Anal. Biochem.* 226:342–48
85. Raether H. 1977. Surface plasma oscillations and their applications. In *Physics of Thin Films*, ed. G Hass, MH Francombe, RW Hoffman, 9:145–261. New York: Academic
86. Raghavan M, Wang Y, Bjorkman PJ. 1995. Effects of receptor dimerization on the interaction between the class I major histocompatibility complex-related Fc receptor and IgG. *Proc. Natl. Acad. Sci. USA* 92:11200–2004
87. Rajaram OV, Sawyer WH. 1996. Characterisation of lipid-protein interactions

using a surface plasmon resonance biosensor. *Biochem. Mol. Biol. Int.* 39:31–39
88. Ramsden JJ, Bachmanova GI, Archakov AI. 1996. Immobilization of proteins to lipid bilayers. *Biosensors Bioelectron.* 11:523–28
89. Ramsden JJ, Schneider P. 1993. Membrane insertion and antibody recognition of a glycosylphosphatidylinositol-anchored protein: An optical study. *Biochemistry* 32:523–29
90. Richalet-Sécordel PM, Zeder-Lutz G, Plaue S, Sommermeyer-Leroux G, Van Regenmortel MHV. 1994. Cross-reactivity of monoclonal antibodies to a chimeric V3 peptide of HIV-1 with peptide analogues studied by biosensor technology and ELISA. *J. Immunol. Methods* 176:221–34
91. Riggs AD, Bourgeois S, Cohn M. 1970. The *lac* repressor-operator interaction. III. Kinetic studies. *J. Mol. Biol.* 53:401–17
92. Sackmann E. 1996. Supported membranes: Scientific and practical applications. *Science* 271:43–48
93. Salamon Z, Tollin G. 1996. Surface plasmon resonance studies of complex formation between cytochrome c and bovine cytochrome c oxidase incorporated into a supported planar lipid bilayer. I. Binding of cytochrome c to cardiolipin/phosphatidylcholine membranes in the absence of oxidase. *Biophys. J.* 71:848–57
94. Salamon Z, Tollin G. 1996. Surface plasmon resonance studies of complex formation between cytochrome c and bovine cytochrome c oxidase incorporated into a supported planar lipid bilayer. II. Binding of cytochrome c to oxidase-containing cardiolipin/phosphatidylcholin membranes. *Biophys. J.* 71:858–67
95. Schmidt A, Spinke J, Bayerl T, Sackmann E, Knoll W. 1992. Streptavidin binding to biotinylated lipid layers on solid supports. *Biophys. J.* 63:1185–92
96. Schmitz KS, Schurr JM. 1972. The role of orientation constraints and rotational diffusion in bimolecular solution kinetics. *J. Phys. Chem.* 76:534–45
97. Schuck P. 1996. Kinetics of ligand binding to receptor immobilized in a polymer matrix, as detected with an evanescent wave biosensor. I. A computer simulation of the influence of mass transport. *Biophys. J.* 70:1230–49
98. Schuck P, Minton AP. 1996. Analysis of mass transport limited binding kinetics in evanescent wave biosensors. *Anal. Biochem.* 240:262–72
99. Schuck P, Minton AP. 1996. Minimal requirements for internal consistency of the analysis of surface plasmon resonance biosensor data. *Trends Biochem. Sci.* 21:458–60
100. Schuster SC, Swanson RV, Alex LA, Bourret RB, Simon MI. 1993. Assembly and function of a quaternary signal transduction complex monitored by surface plasmon resonance. *Nature* 365:343–47
101. Sigal GB, Bamdad C, Barberis A, Strominger J, Whitesides GM. 1996. A self-assembled monolayer for the binding and study of histidine-tagged proteins by surface plasmon resonance. *Anal. Chem.* 68:490–97
102. Silhavy TJ, Szmelcman S, Boos W, Schwartz M. 1975. On the significance of the retention of ligand by protein. *Proc. Natl. Acad. Sci. USA* 72:2120–24
103. Sjölander S, Urbaniczky C. 1991. Integrated fluid handling system for biomolecular interaction analysis. *Anal. Chem.* 63:2338–45
104. Stein T, Gerisch G. 1996. Oriented binding of a lipid-anchored cell adhesion protein onto a biosensor surface using hydrophobic immobilization and photoactive crosslinking. *Anal. Biochem.* 237:252–59
105. Stenberg E, Persson B, Roos H, Urbaniczky C. 1991. Quantitative determination of surface concentration of protein with surface plasmon resonance using radiolabeled proteins. *J. Colloid Interface Sci.* 143:513–26
106. Takano E, Hatanaka M, Maki M. 1994. Real-time analysis of the calcium-dependent interaction between calmodulin and a synthetic oligopeptide of calcineurin by a surface plasmon resonance biosensor. *FEBS Lett.* 352:247–50
107. Tiefenthaler K. 1992. Integrated optical couplers as chemical waveguide sensors. *Adv. Biosensors* 2:261–89
108. van den Heuvel DJ, Kooyman RPH, Drijfhout JW, Welling GW. 1993. Synthetic peptides as receptors in affinity sensors: A feasibility study. *Anal. Biochem.* 215:223–30
109. van der Merwe PA, Barclay AN. 1996. Analysis of cell-adhesion molecule interactions using surface plasmon resonance. *Curr. Opin. Immunol.* 8:257–61
110. van der Merwe PA, Barclay AN, Mason DW, Davies EA, Morgan BP, et al. 1994. Human cell-adhesion molecule CD2 binds CD58 (LFA-3) with a very low

affinity and an extremely fast dissociation rate but does not bind CD48 or CD59. *Biochemistry* 33:10149–60
111. van der Merwe PA, Brown MH, Davis SJ, Barclay AN. 1993. Affinity and kinetic analysis of the interaction of the cell adhesion molecules rat CD2 and CD48. *EMBO J.* 12:4945–54
112. Van Regenmortel MHV, Altschuh D, Pellequer J-L, Richalet-Sécordel P, Saunal H, et al. 1994. Analysis of viral antigens using biosensor technology. *Methods: Companion Methods Enzymol.* 6:177–87
113. Ward LD, Howlett GJ, Hammacher A, Weinstock J, Yasukawa K, et al. 1995. Use of a biosensor with surface plasmon resonance detection for the determination of binding constants: Measurement of interleukin-6 binding to the soluble interleukin-6 receptor. *Biochemistry* 34:2901–7
114. Wu Z, Johnson KW, Choi Y, Ciardelli TL. 1995. Ligand binding analysis of soluble interleukin-2 receptor complexes by surface plasmon resonance. *J. Biol. Chem.* 270:16045–51
115. Yang W-P, Wu H, Barbas CF III. 1995. Surface plasmon resonance based kinetic studies of zinc finger-DNA interactions. *J. Immunol. Methods* 183:175–82
116. Yeung D, Gill A, Maule CH, Davies RJ. 1995. Detection and quantification of biomolecular interactions with optical biosensors. *Trends Anal. Chem.* 14:49–56
117. Zahn R, Axmann SE, Rücknagel K-P, Jaeger E, Laminet AA, et al. 1994. Thermodynamic partitioning model for hydrophobic binding of polypeptides by GroEL. *J. Mol. Biol.* 242:150–64
118. Zimmerman SB, Minton AP. 1993. Macromolecular crowding: Biochemical, biophysical, and physiological consequences. *Annu. Rev. Biophys. Biomol. Struct.* 22:27–65